Comparative Study on Module Connections to Minimize Degradation of Photovoltaic Systems due to Bird Droppings

Chaeyoung Lee[*], Jangwon Suh[**], Yosoon Choi[***‡]

* Department of Energy Resources Engineering, Pukyong National University, Busan, Korea

** Department of Energy and Mineral Resources Engineering, Kangwon National University, Samcheok, Korea

*** Department of Energy Resources Engineering, Pukyong National University, Busan, Korea

(gksthf5971@gmail.com, jangwonsuh@hanmail.net, energy@pknu.ac.kr)

‡ Corresponding Author; Prof. Yosoon Choi, Pukyong National University, Busan 608-737, Korea, Tel: +82 051 629 6562, Fax: +82 051 629 6553, energy@pknu.ac.kr

Received: 15.06.2017 Accepted:24.07.2017

Abstract- Bird droppings on the module surface of photovoltaic (PV) systems significantly reduce the electrical power production owing to their shading effects. However, the removal of bird droppings from the surface is difficult when the PV systems are installed in remote or offshore areas. Toward this aim, this study compared the different methods for connecting PV modules to reduce the degradation of electrical power production of PV systems due to bird droppings. For indoor experiments, 22 module configurations to connect nine modules (3 × 3) in the PV system and six different shading patterns of bird droppings were considered in this study. The results showed that the degradation effects of the PV array with the parallels connected in series were less than the other arrays. Therefore, we could suggest a module configuration method to minimize the degradation of PV systems due to bird droppings.

Keywords Photovoltaic system, Module configuration, Bird droppings, Shading effect, Performance degradation.

1. Introduction

Photovoltaic (PV) systems that can directly convert solar energy into electrical energy can be installed at any place where sunlight is available and has the advantages of being a simple system to operate and maintain [1]. PV systems today are not only used in residential areas, commercial facilities, and large power plants, but are also widely used in polar regions, forests, and marine environments [2, 3]. Recently, several cases of PV system installations on oceanographic observation buoys have been reported [4].

PV systems installed in polar regions, remote areas, and marine environments are difficult to regularly manage and maintain because of their low accessibility. Therefore, it is not easy to clean dirt, dust, and bird droppings from the PV module surface. Bird droppings that include digestive fluids are not cleansed well even by heavy rainfall, which can continuously cause the degradation of the PV system performance (reduction in power production) [5, 6]. Therefore, the possibility of the PV module surfaces being covered by dirt, dust, and bird droppings should be recognized when installing PV systems in polar regions, remote areas, and marine environments and PV systems should be designed to prepare for this possibility.

Various studies have attempted to analyze the degradation of PV system performance that can occur when the PV module surfaces are covered by dirt and dust. Nimmo and Seid [7] proved through experiments that the power production of PV systems can fall to 40% when the PV module surfaces are polluted by dust. Wakim [8] confirmed that the power production of PV systems falls to 17% due to the effect of dirt covering the PV module surfaces for six days. Dorobantu et al. [9] checked the degradation of PV system performance as the internal temperature of the modules increased when foreign substances existed on module surfaces. Rao et al. [10] conducted various experiments in outdoor environments to analyze the degradation of PV system performance due to the effect of dust. Shaharin et al. [11] analyzed the influence of talcum powder, dust, dirt, and moss on PV module surfaces on the decrease of power production through experiments considering various angles of incidence of sunlight.

Because regular maintenance of PV systems installed in polar regions, remote areas, and marine environments is difficult, the system design should be performed by considering the decrease in production when the PV module surfaces are polluted by dirt, dust, and bird droppings. With a similar purpose, research on the connecting methods of PV modules is currently being conducted to reduce the decrease of power production even if partial shadows are formed on the module surface of PV systems. Maki [12] classified all connecting methods of PV systems into three types and analyzed the maximum power point and mismatch loss rate when partial shadows occur on the module surface. In addition, Montano et al. [13] analyzed the current-voltage curves (I-V curve) and power-voltage curves (P-V curve) by applying 16 types of partial shadow patterns using the MATLAB Simulink simulation language. They further suggested a total cross-tied (TCT) shape module connecting method that can reduce the degradation of PV system performance. Patel and Agarwal [14] analyzed the effect of shadows on PV array characteristics through simulations using the MATLAB language.

Existing studies have the following limitations. First, dirt and dust were mainly considered as the pollutants on PV module surfaces whereas the effects of bird droppings on the degradation of PV system performance were not yet analyzed. As installations of systems in oceanographic observation buoys are rapidly increasing for marine environment monitoring, research on the effect of bird droppings on the power production of PV systems is required. Second, previous studies used simulation methods to determine the decrease in power production even if partial shadows or pollution are present on module surfaces. However, different methods other than indoor simulated experiments or field tests should also be applied to verify the actual effects of module connecting methods.

The purpose of this study is to propose an array method for PV module connection that can reduce the decrease of PV system power production due to bird droppings through laboratory-simulated experiments. A scaled model of a PV system composed of nine PV modules (3 × 3) was produced and a total of 37 types of arrays were considered to connect the modules. Moreover, shadow masks that can simulate bird droppings on PV surfaces were classified into three groups (pattern with large bird droppings largely spread around, pattern with sporadic small bird droppings, and pattern with bird droppings spread in an intermediate form of the two previous patterns) and two samples of each group were produced (a total of 6 samples). The reduction rate of power production shown before and after applying shadow masks was quantitatively analyzed. Through a comparison of power production reduction rate in accordance with all the connection arrays, a method to connect the modules is proposed to minimize the reduction in power production even if bird droppings fall on the PV module surfaces.

2. Methodology

Experiments on methods to connect modules to reduce the degradation of PV system performance due to bird droppings were performed in four steps as shown in Fig. 1. In the first step, the number of cases of arrays in the nine modules (three horizontal, three vertical) was calculated by considering the number of PV system modules used in the experiments. The number of cases was calculated by assuming combinations without overlapping and consideration for the repetition or order of the module arrays because the effect of bird droppings is random. Among the module arrays, those with a potential difference due to parallel connections were excluded.

In the second step, photos of actual bird droppings were used to create the shadow masks. In the third step, bird dropping shadow patterns were applied to each module connection array that was designed in the first step to measure the I-V curves. These curves also were measured for cases without bird dropping shadow patterns. In the last step, to select the optimal array, the reduction rates of the PV system power production that receive the effect of bird droppings were comparatively analyzed with the measured I-V curves depending on the existence of bird dropping shadows. Detailed explanations of each step are presented in the following sub-sections.

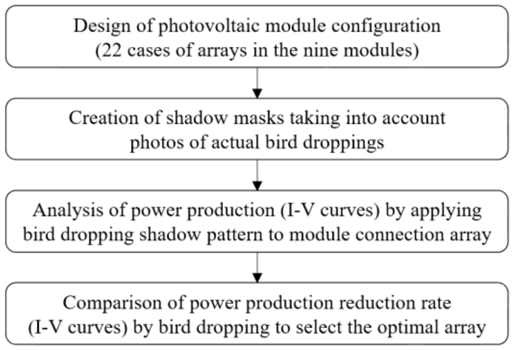

Fig. 1. Flow chart of experimental procedure to determine the best module configuration.

2.1 Design of Connection Array of PV Module

The scaled PV system that was manufactured in this study is composed of nine PV modules in a 3 × 3 form. There are a total of 9! possible array configurations to connect the modules in this system. However, the order and repetition were not considered in the module connection arrays because the position of bird droppings on the PV modules was random. For example, Fig. 2a and 2b are assumed to be equivalent connection arrays.

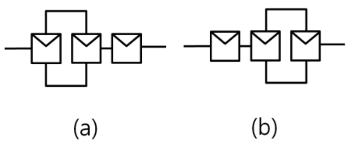

Fig. 2. Example of equivalent patterns for connecting PV modules.

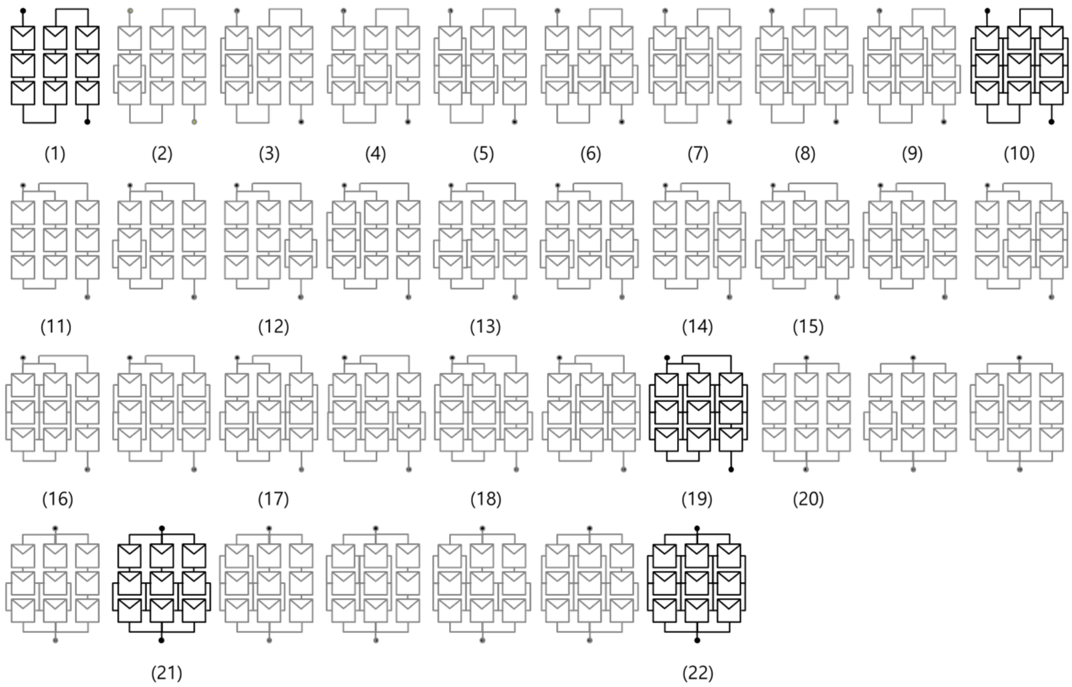

Fig. 3. Module configurations considered in this study. The 22 PV module configurations without loss due to a potential difference are shown with the ID. The final 5 module configurations were represented by black color.

A total of 37 types of connection arrays of the 3 × 3 array could be designed in module configurations without repetition (Figure 3). Fifteen types of connection arrays that can exhibit power loss due to the voltage difference between the serial and parallel connection voltage were excluded from the test subjects. Therefore, 22 types of PV system module configurations were considered in this study (Fig. 3).

2.2 Production of Shadow Masks using Photos of Actual Bird Droppings

Photos of actual bird droppings on the surface of PV modules installed at various sites were taken to create shadow masks that mimic bird droppings. Three main types of patterns were extracted through the analysis of various forms of bird droppings from the photos. The three patterns were: (1) large and spread pattern, (2) small and sporadic pattern, and (3) medium and scattered pattern (Fig. 4). Two forms of actual bird droppings for each pattern were printed on an overhead projector (OHP) film to create six shadow masks. OHP films with bird dropping shapes were created as white and black shadows, and two films were overlapped to prevent light penetrating the printed film. This work was performed to equivalently measure the light transmission rate according to the film thickness. In addition, the two films without bird dropping shadow patterns were attached with the same method above to calculate the reduction rate of the PV system production affected by bird droppings.

2.3 Analysis of Power Production by Applying Bird Dropping Shadow Masks to Each Module Configuration

Nine 0.3 W PV modules (three horizontal, three vertical) were created in this study for the test equipment. The light source (and module angle) was designed to be adjusted (Fig. 5). The specification of the nine PV modules used in this study is shown in Table 1. The I-V and P-V curves of the PV systems according to the module connection methods and the application of shadow masks were measured at an luminance of 1000 W/m^2 and a temperature of 25℃ according to the standard test conditions in this study. The image of the connection using wires on the back side of the module is shown in Figure 6. The serial connection (+) pole of one module connected with – pole of other modules) is shown in Fig. 6a and the parallel connection is shown in Fig. 6b (+) pole and (–) pole of each module connected to each other).

2.4 Calculation of Power Production Reduction Rates according to the Bird Dropping Shadow Masks

The maximum power without shadow masks was set as the standard value and the reduction of power production according to the shadow mask application was calculated with Eq. (1), considering the power production when applying the shadow masks.

$$\frac{P_{i,max}(\text{without mask}) - P_{i,max}(\text{with mask})}{P_{i,max}(\text{without mask})} \times 100(\%) \qquad (1)$$

Here, the reduction rate is defined as the rate of difference between the maximum power of the i-th array without the shadow mask effect and that with the shadow mask effect normalized to that without the shadow mask effect. To calculate the reduction rate of the power production, 22 types of module connection arrays and six types of shadow masks were applied.

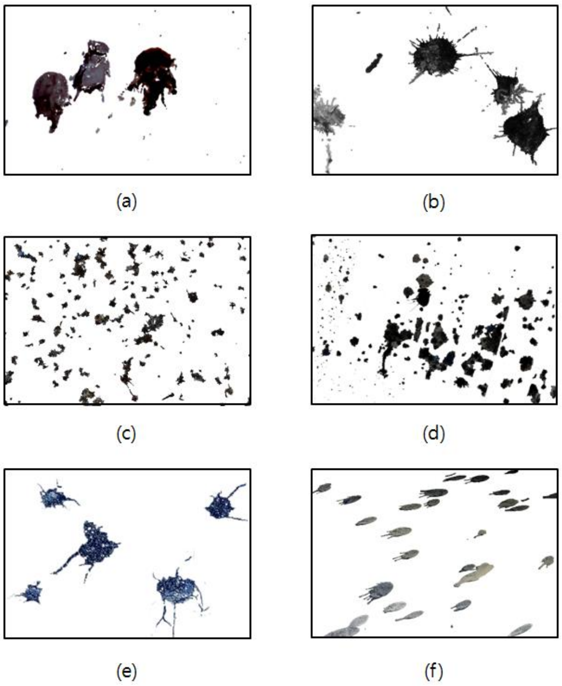

Fig. 4. Shadow masks representing the bird droppings on photovoltaic modules. (a) Large and spread pattern 1, (b) large and spread pattern 2, (c) small and sporadic pattern 1, (d) small and sporadic pattern 2, (e) medium and scattered pattern 1, and (f) medium and scattered pattern 2.

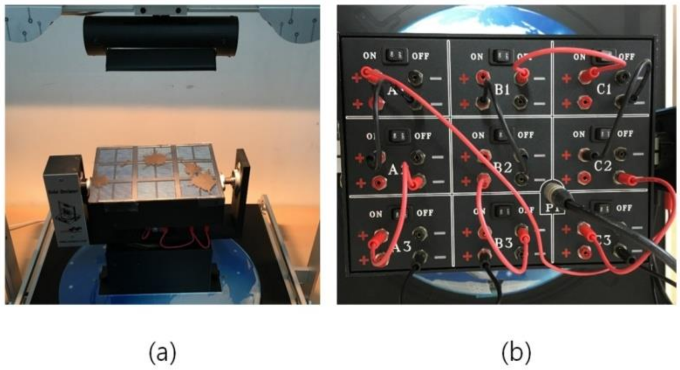

Fig. 5. Experimental equipment. (a) Photovoltaic modules with shading mask representing bird droppings. (b) Connected photovoltaic modules with wires.

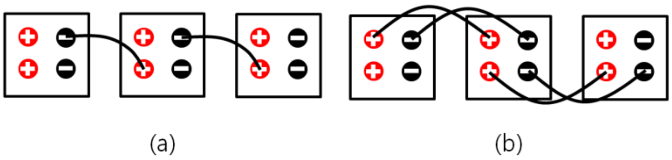

Fig. 6. Schematic diagram showing (a) series connection of modules and (b) parallel connection of modules.

Table 1. Specification of each photovoltaic module used in this study.

Module number	V_{oc}[1] (mV)	I_{sc}[2] (mA)	V_{max}[3] (mV)	I_{max}[4] (mA)	P_{max}[5] (mW)	R_s[6] (Ω)	R_{sh}[7] (Ω)	FF[8]
1	1752.1	65.4	1405.1	54.9	77.0	2.5	227.4	0.7
2	1749.4	69.3	1368.4	57.2	78.2	2.6	199.8	0.6
3	1747.8	62.0	1401.7	48.8	69.3	2.6	104.6	0.6
4	1782.3	68.8	1315.1	47.7	63.3	4.3	82.1	0.5
5	1786.0	71.9	1283.1	532.0	67.7	5.6	1052.9	0.5
6	1750.6	64.4	1386.6	49.4	69.4	3.1	91.9	0.6
7	1766.8	43.1	1406.6	37.9	53.5	5.0	5075.8	0.7
8	1736.7	69.6	1392.8	59.1	82.4	2.3	258.4	0.7
9	1832.1	59.2	1326.1	46.0	61.2	12.7	179.3	0.6

[1]Open circuit voltage, [2]Short-circuit current, [3]Maximum voltage, [4]Maximum current, [5]Maximum electric power, [6]Internal series resistance, [7]Internal parallel resistance, [8]Fill factor.

3. Results and Discussion

The maximum power from six types of data with bird dropping shadow patterns by the configuration method and one type of data with the mask without the bird dropping pattern were obtained through the I-V curve measurements (Table 2). A different maximum power was measured according to the module configuration.

A1–C2 are the test results attaching the masks that have shadow patterns and D is the test result attaching the mask without the shadow pattern. As seen in the test results, module configuration 17 showed a power that was substantially lower than the other configurations. This low power is considered to be due to module resistance problems because of the low internal serial resistance within the module (R_{sh}) or the high internal parallel resistance (R_s). It also could be due to the changing of the R_{sh} and R_s values or the voltage difference between the modules with or without bird dropping shadow patterns. It was judged that the module configurations that show the maximum power production higher than the maximum power production of the module configurations that are serially connected (number 1 of Figure 3 and Table 2) suited the power efficiency standard. As a result, a total of five module configurations that satisfy the power efficiency standard (number 1, 10, 19, 21, 22) were selected and schematic diagrams of each module configuration are shown in Fig. 3.

Fig. 7 shows the measured I-V and P-V curves of each module configuration that vary according to the bird dropping shadow patterns. It can be seen in Fig. 7 that the power decreases when the PV module is affected by the bird droppings. The calculated power production and reduction rate before and after applying the shadow masks on the configurations with a power production higher than the configuration only connected in parallel (number 10, 19, 21, 22) compared to that only connected in series (number 1) are shown in Table 3.

The module configuration that showed the lowest mean reduction rate owing to the six types of bird dropping shadow patterns was number 10 (configuration connecting three parallel-connected modules in series, 15.51%). Considering that the index deviation of the reduction rate was 5.84%, which was relatively small, it is interpreted that the effect of bird dropping shadow patterns is relatively evenly shown. The mean reduction rate of module configuration 19 was similar to configuration 10, but the standard deviation of the reduction rate was 7.95%, which is 2.11% higher. This implies that there is a higher probability of the reduction rate varying depending on the bird dropping shadow pattern. Therefore, it was found that configuration number 10, which showed the lowest reduction rate index and standard deviation among the 22 module configurations while also satisfying the power efficiency standard, is the module configuration that can minimize the degradation of system performance among the module connection methods reviewed in this study.

Table 2. The result of maximum electrical power productions from 22 module configurations depending on different shading patterns of bird droppings.

ID of module configuration method	A1 (large and spread pattern 1, mW)	A2 (large and spread pattern 2, mW)	B1 (small and sporadic pattern 1, mW)	B2 (small and sporadic pattern 2, mW)	C1 (medium and scatter pattern 1, mW)	C2 (medium and scatter pattern 2, mW)	D (without bird droppings, mW)
1	201.47	211.14	288.91	276.91	285.98	288.91	319.48
2	189.68	205.26	293.70	240.45	279.57	267.05	316.36
3	200.36	212.14	276.20	232.06	298.15	272.34	314.18
4	209.26	289.04	268.43	305.41	271.99	292.67	309.37
5	185.71	187.95	262.40	279.59	269.56	260.45	308.48
6	194.13	273.74	271.44	279.32	268.26	266.26	314.92
7	162.26	191.95	233.85	285.74	282.4	288.91	314.69
8	197.61	245.91	262.28	287.72	277.46	266.79	310.69
9	169.11	260.92	240.83	247.69	236.20	243.15	263.91
10	374.75	393.27	425.32	382.37	443.71	428.56	482.93
11	160.03	161.03	213.46	189.08	216.67	216.10	236.62
12	139.31	182.18	169.48	155.35	168.38	163.21	209.18
13	98.92	76.27	94.50	86.01	100.64	97.36	105.01
14	96.47	129.78	149.80	107.96	140.23	142.72	164.61
15	59.13	56.40	47.96	56.12	57.83	55.18	61.74
16	168.98	162.75	216.96	197.93	220.20	221.84	249.96
17	3.13	2.71	3.51	2.42	3.03	3.72	3.92
18	120.93	185.49	180.41	185.76	178.03	180.82	195.78
19	244.65	256.27	294.21	258.57	308.00	294.50	326.74
20	89.07	146.81	146.60	132.43	144.67	142.22	152.37
21	304.66	315.34	329.45	286.62	344.48	326.34	384.74
22	339.45	339.45	322.45	303.44	342.74	338.50	403.82

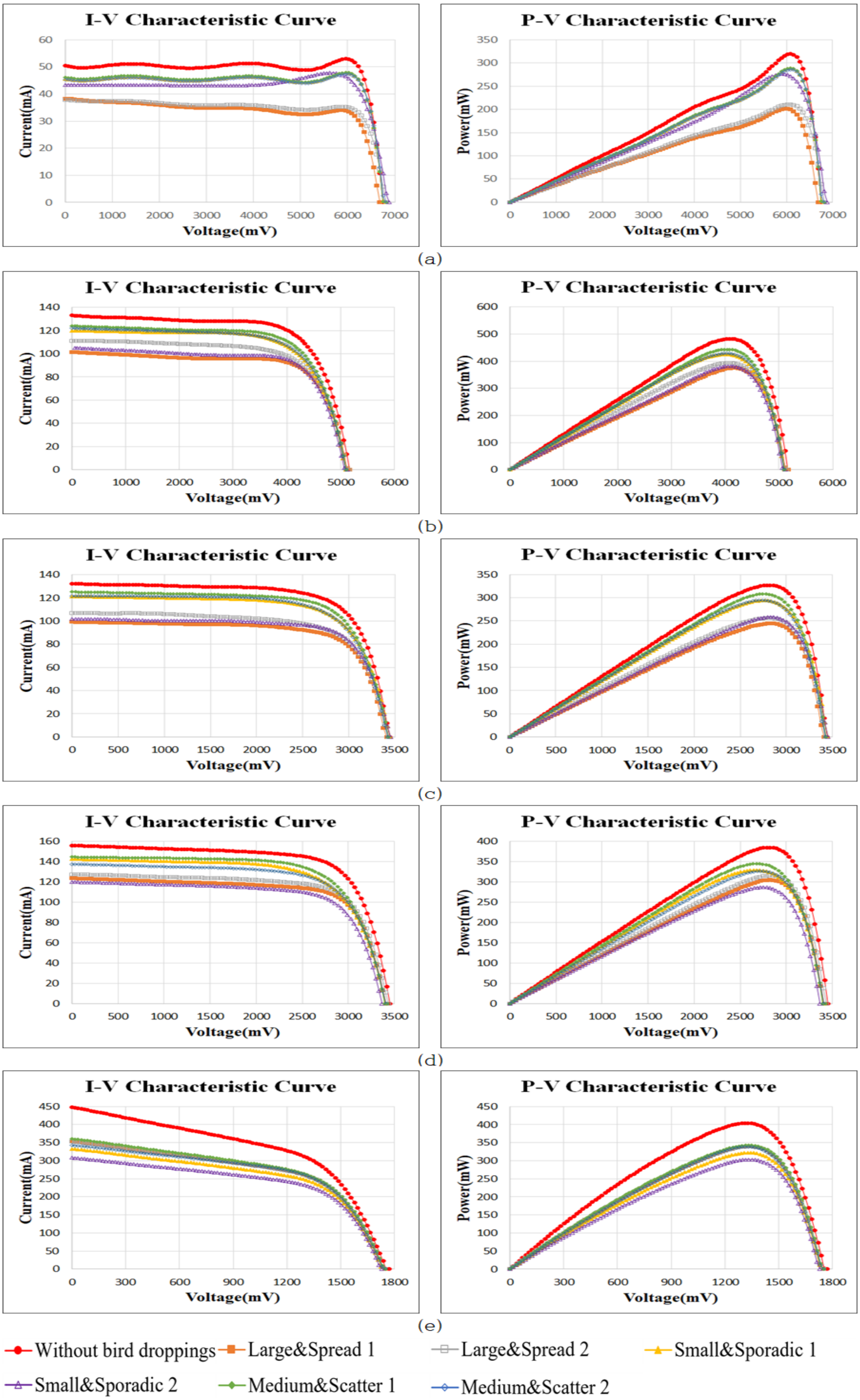

Fig. 7. Current-voltage (I-V) and power-voltage (P-V) curves measured from configuration ID (a) 1, (b) 10, (c) 19, (d) 21, and (e) 22.

Table 3. Results from the five different module configurations.

ID	ID of the module configuration method (%)									Power (mW)
	A1 (large and spread pattern 1)	A2 (large and spread pattern 2)	B1 (small and sporadic pattern 1)	B2 (small and sporadic pattern 2)	C1 (medium and scatter pattern 1)	C2 (medium and scatter pattern 2)	Average	Ave. rank	Standard deviation	D (without bird droppings)
1	36.94	33.91	9.57	13.33	9.50	10.49	18.95	5	12.87	319.48
10	22.40	18.57	11.93	20.82	8.12	11.26	15.51	1	5.84	482.93
19	25.12	21.57	9.96	20.87	5.74	9.87	15.52	2	7.95	326.74
21	20.81	18.04	14.37	25.50	10.47	15.18	17.39	3	5.30	384.74
22	15.94	15.94	20.15	24.86	15.13	16.18	18.03	4	3.79	403.82

4. Conclusion

Shadow patterns of actual bird droppings were applied in this study, and laboratory-simulated experiments were conducted to compare module configurations. As a result, module configuration number 10 showed a mean reduction rate index of 15.51% and a standard deviation of 5.84%, which was considered to be the configuration that could minimize the degradation of PV system performance when affected by bird droppings. It is considered that this configuration can be applied to actual sites as the connecting method is not complicated.

There have been many studies on experiments creating partial shadows or module configurations with simulations [15-22]. Moreover, experiments or simulation tests on the power loss of PV systems affected by partial shadows of pollutants such as dust, dirt, and moss were performed. This study is distinctive from existing research because shadows of bird droppings, which was not researched as a pollutant, were used in a scaled PV system.

PV systems are not only installed in everyday life, but are also installed on the top of mountains or oceanographic observatory buoys that are difficult to access [23-24]. Regular management and maintenance are difficult in these PV systems that are installed in these remote areas. Bird droppings that contain digestive fluids cannot be cleansed by heavy rain in which this effect is very important. Therefore, the possibility of PV module surfaces being covered by dirt, dust, and bird droppings must be recognized and prepared for by design when installing PV systems in polar regions, remote areas, and marine environments. It is considered that the results of this study can help in determining the module configurations in the field.

Acknowledgements

This work was supported by a Research Grant of Pukyong National University (2017 year).

Abbreviations

Fill factor	FF
Internal parallel resistance	R_{sh}
Internal series resistance	R_s
Maximum current	I_{max}
Maximum electric power	P_{max}
Maximum voltage	V_{max}
Open circuit voltage	V_{oc}
Short-circuit current	I_{sc}

References

[1] Park, H., Choi, Y., Hyun, C. U., Suh, J., Park, J. H., Renewable Energy 2nd ed., CIR Press, 2012, pp. 3–17.

[2] Suh, J., Brownson, J. R. S., "Solar farm suitability using GIS fuzzy sets and analytic hierarchy processes: Case study of Ulleung Island, Korea", Energies, Vol. 9, pp. 648–671, August 2016

[3] Song, J., Choi, Y., "Analysis of the Potential for Use of Floating Photovoltaic Systems on Mine Pit Lakes: Case Study at the Ssangyong Open-Pit Limestone Mine in Korea", Energies, Vol. 9, pp. 102-114, February 2016

[4] Behrouzian, E., Tabesh, A., Bahrainian, F., Zamani, A., "Power Electronics for Photovoltaic Energy System of an Oceanographic Buoy", Applied Power Electronics Colloquium (IAPEC), IEEE 2011, pp. 1–4, 18-19 April 2011.

[5] Mani, M., Pillai, R., "Impact of dust on solar photovoltaic (PV) performance: Research status, challenges and recommendations", Renewable and Sustainable Energy Reviews, Vol. 14, pp. 3124–3131, December 2010.

[6] Kumar, E. S., Sarkar, D. B., Behera, D. K., "Soiling and Dust Impact on the Efficiency and the Maximum Power Point in the Photovoltaic Modules", International Journal of Engineering Research & Technology (IJERT), Vol. 2, pp. 1–8, February 2013.

[7] Nimmo, B., Seid, S. A. M., "Effects of dust on the performance of thermal and photovoltaic flat plate collectors

in Saudi Arabia: Miami Beach”, Proceedings of Second Miami International Conference, Vol. 1, pp. 145–152, December 1979.

[8] Wakim, F., “Introduction of PV power generation to Kuwait”, Kuwait Institute for Scientific Researchers, 1981.

[9] Dorobantu, L., Popescu, M.O., Popescu, CL., Craciunescu, A., “The effect of surface impurities on photovoltaic panels”, Proceedings of International Conference on Renewable Energies and Power Quality (ICREPQ’11), Spain, pp. 622-626, 13-15 April 2011.

[10] Rao, A., Pillai, R., Mani, M., Ramamurthy, P., “Influence of dust deposition on photovoltaic panel performance”, Proceedings of 4th International Conference on Advances in Energy Research 2013 (ICAER2013), Vol. 54, pp. 690–700, 2014.

[11] Sulaiman, S. A., Singh, A. K., Mokhtar, M. M. M., Bou-Rabee, M. A., “Influence of Dirt Accumulation on Performance of PV Panels”, Proceedings of the International Conference on Technologies and Materials for Renewable Energy, Environment and Sustainability (TMREES14), Vol. 50, pp. 50–56, 2014.

[12] Maki, A., “Power Losses in Long String and Parallel-Connected Short Strings of Series-Connected Silicon-Based Photovoltaic Modules Due to Partial Shading Conditions”, IEEE TRANSACTIONS ON ENERGY CONVERSION, Vol. 27, pp. 173–183, March 2012.

[13] Montano, B.J.G., Rombaoa, D.J.F., Pena, R.A.S., Macabebe, E.Q.B., “Effects of Shading on Current, Voltage and Power Output of Total Cross-Tied Photovoltaic Array Configuration”, Proceedings of TENCON 2015 – 2015 IEEE Region 10 Conference, Macao, China, pp. 1-5, November 2015.

[14] Patel, H., Agarwal, V., “MATLAB-Based Modeling to Study the Effects of Partial Shading on PV Array Characteristics”, IEEE Transactions on Energy Conversion, Vol. 23, pp. 302–310, March 2008.

[15] Mochizuki, Y., Yachi, T., “Relationship between power generated and series/parallel solar panel configurations for 3D Fibonacci PV modules”, Proceedings of 2017 IEEE 6th International Conference on Renewable Energy Research and Applications (ICRERA), pp. 126–130, November 2017.

[16] Adachi, T., Obara, S., Kawae, O., “Study on the light receiving capacity of a plant shoot light receiving system with simulated trees”, Proceedings of 2015 International Conference on Renewable Energy Research and Applications (ICRERA), pp. 489–494, November 2015.

[17] Cataliotti, A., Miceli, R., Di Cara, D., Marsala, G., Pecoraro, A., Ragusa, A., Tinè, G., “Electric and magnetic emission in near field region and thermal behaviour of power module for photovoltaic application”, Proceedings of 2015 International Conference on Renewable Energy Research and Applications (ICRERA), pp. 221–226, November 2015.

[18] Balato, M., Costanzo, L., Vitelli, M., “Multi-objective optimization of PV arrays performances by means of the dynamical reconfiguration of PV modules connections”, Proceedings of 2015 International Conference on Renewable Energy Research and Applications (ICRERA), pp. 1646–1650, November 2015.

[19] Andriollo, M., Bortot, F., Tortella, A., “Disc-type PM machine for the electromagnetic conversion/suspension of a flywheel system”, Proceedings of 2015 International Conference on Renewable Energy Research and Applications (ICRERA), pp. 739–744, November 2015.

[20] Saha, S., Akter, S., Mahto, K. K., Das, P., Chakraborty, A. K., Awasthi, G. K., “Improvement in power efficiency of photovoltaic array under shading condition using bypass diode”, International Journal of Renewable Energy Research, Vol. 6, pp. 627–636, June 2016.

[21] Ben cheikh el hocine, H., Touafek, K., Kerrour, F., Khelifa, A., Tabet, I., Haloui, H., “A Three-Dimensional Modeling of Photovoltaic Thermal Collector”, International Journal of Renewable Energy Research, Vol. 6, pp. 384–391, June 2016.

[22] Dayou, J., Man Sang, C., “Performance Study of Piezoelectric Energy Harvesting to Flash A LED”, International Journal of Renewable Energy Research, Vol. 1, pp. 323–332, December 2011.

[23] Choi, Y., Lee, C., Song, J., “Review of Renewable Energy Technologies Utilized in the Oil and Gas Industry”, International Journal of Renewable Energy Research, Vol. 7, pp. 592–598, June 2017.

[24] Choi, Y., Song, J., “Review of photovoltaic and wind power systems utilized in the mining industry”, Renewable and Sustainable Energy Reviews, Vol. 75, pp. 1386-1391, August 2017.